Journal of Population Therapeutics & Clinical Pharmacology

RESEARCH ARTICLE
DOI: 10.53555/jptcp.v30i19.3571

IN SILICO ANALYSIS AND MOLECULAR DOCKING OF CURCUMIN ANALOGS AND ANTIFUNGAL COMPOUNDS AGAINST CRITICAL PROTEINS OF ASPERGILLUS SPECIES: A COMPARATIVE INVESTIGATION

Mohammad Javad Javid-Naderi[1], Hossein Zarrinfar[2*], Tahany Al-Shemary[3]

[1]Department of Medical Biotechnology and Nanotechnology, Faculty of Medicine, Mashhad University of Medical Sciences, Iran
[1]Student Research Committee, Faculty of Medicine, Mashhad University of Medical Sciences, Mashhad, Iran
[2*]Allergy Research Center, Mashhad University of Medical Sciences, Mashhad, Iran
[2]Sinus and Surgical Endoscopic Research Center, Department of Otorhinolaryngology Mashhad University of Medical Sciences Mashhad Iran
[3]Department of Microbiology, College of Medicine, Kuwait University, Jabriya, Kuwait

***Corresponding Author:** Hossein Zarrinfar, PhD
*Allergy Research Center, Laboratory of Parasitology and Mycology, Ghaem Hospital, Mashhad University of Medical Sciences, Mashhad, Iran Phone: +985138403141, Fax: +985138547255; Orcid.org/0000-0002-1449-4668 E-mail: zarrinfarh@mums.ac.ir; h.zarrin@gmail.com

Abstract

Aspergillosis is a range of infections caused by fungi from the *Aspergillus* genus. *Aspergillus* is a common filamentous fungus that primarily infects individuals with compromised immune systems or underlying pulmonary conditions. The clinical manifestations of aspergillosis vary depending on the patient's immune status, with invasive forms predominantly affecting immunocompromised individuals. In recent years, there has been a notable increase in the emergence of *Aspergillus* strains resistant to azole antifungals, particularly within the *A. fumigatus*. After a comprehensive literature review, this research studied six essential proteins that increase resistance in *Aspergillus* species. *In silico* homology modeling and molecular docking with SWISS-MODEL and Autodock Vina in PyRx assessed the inhibitory activity of candidate drugs against these proteins. Toxicity, Drug-likeness, and ADME analysis were evaluated with ProTox-II, pkCSM, StopTox and SwissADME, respectively. The pharmacological activities were predicted by PASS and Molinspiration servers. The ligands of pramiconazole, curcumin difluorinated (CDF), and curcumin exhibited a high binding affinity, indicating their potential to inhibit the overexpression of target proteins. These compounds demonstrated enhanced medicinal attributes and reduced toxicity compared to usual antifungals against *Aspergillus*. Consequently, they can become a promising alternative for overcoming antifungal resistance and treating aspergillosis.

Keywords: *Aspergillus*, Curcumin analogs, Molecular docking, Virtual screening, ADMET

Introduction:

Aspergillus species are the most prevalent fungal agents associated with fatal illnesses, and their infections are a significant public health concern (1, 2). The ability of certain species within the genus to create valuable metabolites has led to their biotechnological usage in the pharmaceutical and industrial sectors (3). However, a wide variety of clinical presentations are observed in *Aspergillus* infections, from skin infections leading to cutaneous aspergillosis to allergy syndromes to persistent pulmonary diseases and invasive infections (4-6). Even though the diagnosis and treatment of aspergillosis have come a long way, it is still hard to avoid and treat severe fungal diseases in hospitals. Death rates remain high, especially among patients with low immune systems with invasive fungal infections (7). *A. fumigatus*, *A. niger*, *A. flavus*, *A. nidulans*, and *A. terreus* are the most commonly reported pathogens globally for various clinical presentations of aspergillosis (8, 9). Antifungal agents have some side effects such as toxicity, drug-drug interactions, varying pharmacokinetics, and fewer bioavailability agents (10). Azoles are the antifungal drugs of choice for curing *Aspergillus* infections because of their high therapeutic index (11). Due to a lack of new antifungal drugs and substantial treatment resistance, invasive fungal infections have a high incidence and mortality rate. Hence, Novel antifungal agents with anti-resistance properties are required to solve these issues (12, 13). First-line treatments for invasive *Aspergillus* are usually voriconazole and isavuconazole, which are reported to have a low success rate (14). These antifungal drugs are associated with adverse effects such as hepatotoxicity, vomiting, vision abnormalities, skin rashes, abdominal pain, etc. Therefore, continual drug monitoring is required for their use. In addition, synthetic fungicides have been called into question due to environmental concerns, and many plant infections are developing resistance to these chemical fungicides (15). Therefore, finding new compounds to treat fungal infections that have more potent antifungal properties with fewer adverse effects is an essential need (16). Several investigations have demonstrated the antifungal effects of various plant-derived compounds (17-19). These plants are regarded as an essential source for identifying new antifungal medication leads, and the traditional herbal therapy strategy is preferred due to fewer side effects and higher efficacy (20). Polyphenols are phytochemicals that inhibit various fungal infections through plasma membrane rupture, suppression of cell walls and protein/DNA/RNA production, and mitochondrial dysfunction (21). Curcumin, as turmeric's active ingredient, has been studied extensively because of its health benefits. Several studies have shown that this compound works well as an antioxidant, an anti-inflammatory, an antibacterial, an antifungal, and an antiviral agent. However, the antifungal potential of curcumin analogs has yet to be thoroughly examined (22-25). Recent research indicates that triazole-based antifungal efficacy relies on reactive oxygen species. Therefore, compounds with antifungal properties, such as curcumin analogs and derivatives, can produce new antifungal drugs (26). Making a new drug in today's scientific world is a complicated process that takes time, money, and people. Therefore, *in silico* techniques have become one of the critical parts of the drug development process (27). Current published studies have used bioinformatics-based virtual screening because it can speed up drug target selection, drug candidate screening and refining, improve the identity of adverse effects, and forecast drug resistance (28, 29). Literature review shows that triazole resistance in *Aspergillus* species is associated with the upregulation of Cyp51A and Cyp51B enzymes and the efflux pumps (MDR1, MDR2, MDR3, and MDR4). Therefore, it is necessary to investigate their structure and function in detail and based on a bioinformatics approach, which provides unique insight into developing effective, inexpensive, and side-effect-free drugs (30). The present examination goal of this study is to gather about 100 compounds (antifungal agents and their similar structures, curcumin and its analogs) with antifungal and antimicrobial properties. The compounds were chosen from articles and scientific reports. Then, they were evaluated using an *in silico* approach, which involved protein modeling, molecular docking, drug-likeness assessment, and prediction of chemical absorption, distribution, metabolism, and excretion (ADME), toxicity, and biological activity against essential *Aspergillus* proteins, including Cyp51A and Cyp51B enzymes, as well as efflux pumps (MDR1-4). The diagram of the overall steps and the methodology applied in the present study is displayed in **Fig.1.**

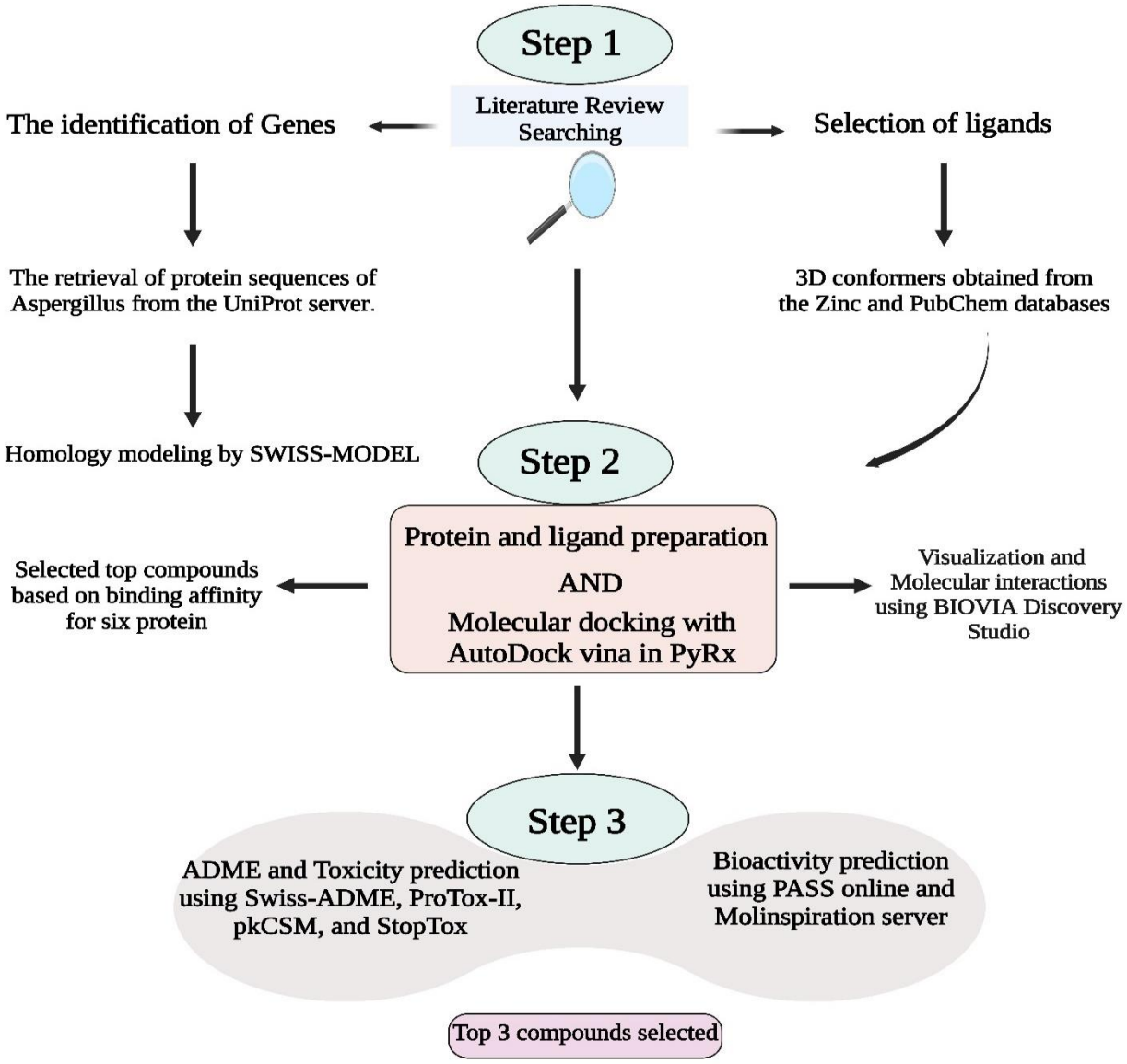

Fig. 1. A diagram illustrating the overall steps in the current study.

2. Methods

2.1 Protein Preparation

The sequence of the target proteins in *Aspergillus* spp. including (Cyp51A, Cyp51B, MDR1, MDR2, MDR3, and MDR4) was obtained through the UniProt dataset. The UniProt is a comprehensive repository of protein sequences accompanied by extensive annotations (31). The 3D structure of Cyp51B (PDB code 5FRB) was retrieved from the Protein Data Bank (PDB), the world's only repository for structural data on biological macromolecules. It comprises NMR spectrometry and X-ray crystallography data from biologists and biochemists worldwide (32). However, because the 3D crystal structures of Cyp51A, MDR1, MDR2, MDR3, and MDR4 were not accessible, they were built using homology modeling. This modeling was done using the SWISS-MODEL service and was based on genomic sequences (33). SWISS-MODEL is a Web-based, completely automated homology modeling server. Homology modeling is started by entering the target sequence in the SWISS-MODEL server. Following the selection of templates from a list provided by the system, all subsequent stages in homology modeling are carried out automatically (34). Several 3D protein structures with high similarity were considered templates to build the 3D structure of target proteins.

2.1.1 Identification of Physiochemical Properties

The ProtParam tool, available on the ExPasy server, was utilized to determine various protein properties such as Molecular Weight (MW), Isoelectric point, Amino acid composition, half-life prediction, stability index, aliphatic index, and GRAVY (35). The Instability Index is a metric that can be utilized to assess the stability of a protein in vitro (36). The aliphatic index of a protein refers to the proportion of its overall volume comprising its aliphatic side chains. The hypothesis posits that this phenomenon enhances the thermal stability of proteins with a globular structure (37). Peptide and protein GRAVY values are calculated by adding the hydropathy scores of each amino acid and then dividing by the total number of residues (38).

2.1.2 Model Validation for Proteins

Models were validated using the SAVES v6.0 server, which compares predictions for stereochemical protein structural parameters using the ERRAT, Verified 3D, and Ramachandran plots. Stereochemical characteristics and model quality were evaluated using Ramachandran and ERRAT plots (39). The Ramachandran plot can be used to predict the stereochemical feature of a given structure. The Verify3D employs protein structural database data to assess the compatibility of a 3D model with a 1D amino acid sequence based on structural assignments such as loops, sheets, alpha-helix, and other related factors (40).

2.2 Ligand Preparation

Twenty routinely prescribed antifungal drugs were examined (such as voriconazole, amphotericin B, itraconazole, fluconazole, ketoconazole, miconazole, isoconazole**,** oteseconazole, quilseconazole isavuconazole**,** caspofungin, micafungin, anidulafungin, nystatin, nikkomycin, terbinafine, 5-fluorocytosine, luliconazole, posaconazole, and efinaconazole). Similar structures (with similarity threshold (≥ 0.7)) compared with curcumin and its analogs *in silico* study. The smiles sequences of the structure antifungal drugs and similar structures, as well as curcumin in a single structure document (SDF) format, were obtained from the Zinc 15 and PubChem server. ZINC is an open-access dataset that can be used to find new ligands. Over 20 million commercially accessible compounds are stored in the database with biologically appropriate representations that may be downloaded in standard ready-to-dock formats and subsets (41). PubChem is a database of chemicals and the biological processes they undergo (42). Additionally, compounds were ready and transformed into the dockable PDBQT (Protein Data Bank, Partial Charge (Q), and Atom Type (T)) format via Autodock Vina in PyRx 0.8 software.

2.3. Molecular Docking

The antifungal effects of the compounds were evaluated using two computational methodologies, namely homology modeling and molecular docking. Homology modeling uses similar templates to construct a three-dimensional protein structure from a protein sequence (43). Molecular docking is a promising technique for conducting virtual screening on numerous compounds and understanding whether ligands interact with their targets (44). PyRx-virtual screening software was used to dock the ligands to the selected proteins and calculate their affinity for binding. PyRx is an open-source tool for docking small-molecule libraries to macromolecules to identify lead compounds (chemical compounds potentially becoming novel medications) with the required biological function (45).

2.4. Molecular Docking Process

In the initial step, the structure of macromolecules was optimized using the UCSF Chimera software (version 1.8.1) by rectifying bonds, deleting irrelevant chemical complexes, removing water molecules, adding hydrogen bonds, and saving to PDBQT format. The resulting 3D structure of proteins was then docked against authorized antifungal medicines, similar structures, and curcumin using the PyRx software. UCSF Chimera is cutting-edge software for visualizing and analyzing molecular structures and data (46).

2.5 Visualization and Molecular Interactions

Several top intersection outcomes among all protein targets were chosen based on binding energies (ΔGbind), and their interactions were examined using BIOVIA Discovery Studio Visualizer, 2016. Discovery Studio Visualize is a free molecular modeling program that enables researchers to see, exchange, and analyze data from proteins and small molecules (47).

2.6 Drug-Likeness Features Evaluation and ADME Evaluation

ADME studies are paramount in contemporary pharmaceutical research and development. Early detection of these features is critical for successful drug discovery research since it allows molecules with undesirable pharmacokinetic properties to be eliminated. *In silico* ADME and toxicological screening methods can help forecast performance in a real-world environment. Further, using the SwissADME server, the pharmacokinetic profiles of the top 10 drugs and curcumin could be predicted by entering their SMILES. The SwissADME anticipated outcome comprises water solubility, pharmacokinetics, bioavailability score, and drug-likeness properties (48). In addition, SwissADME was used to determine the drug-like features of each compound. The physicochemical features of small molecule medications have a substantial effect on their permeability, mainly via passive diffusion. Following Lipinski's "rule of five," molecules should have a molecular weight (MW) below 500, several hydrogen bond donors (HBD) below 5, several hydrogen bond acceptors (HBA) below 10, and a consensus log p-value (log p) below five (49). Fulfilling these standards does not guarantee the oral bioavailability of a compound. Consequently, further explorations were conducted on additional attributes of drug-likeness, encompassing the topological polar surface area (TPSA≤ 140) with a maximum value of 140 and the count of rotatable bonds (RB ≤ 10) not exceeding 10. These parameters could provide more precise approximations of the probability of activity. The top ten compounds (based on docking score) were used to predict their drug-like potential by examining pharmacokinetic and pharmacodynamic properties.

2.7 Prediction of Toxicity

The compounds were evaluated initially for toxicity using the ProTox-II and pkCSM servers (50, 51). Toxicology classifications and LD50 values in mg per kg of body weight were obtained from the ProTox-II virtual laboratory. Hepatotoxicity, AMES toxicity, and the human Maximum Tolerable Dose (log mg/kg/day) were all evaluated using the pkCSM server. A compound is hepatotoxic if it causes at least one pathological or physiological change in the liver that is directly linked to a change in how the liver functions (52). The maximum tolerated dose of a chemical is defined as the highest dose that may be given to animals without causing significant toxicity or mortality. The AMES test is a commonly utilized method for determining the mutagenic potential of a substance using microorganisms (53). In addition, the acute toxicity of the compounds was evaluated using the cutting-edge and user-friendly StopTox software program (54).

2.8 Prediction of Pharmacological and Biological Activity

The PASS web server was used for predicting the activity spectrum of compounds. This program assesses a compound's biological potential based on its structure-activity relationship (55). PASS results are presented as a list of potential biological activities with an associated probability of activity (Pa) or inactivity (Pi). The top compounds' bioactivity profiles were estimated using the Molinspiration website (56).

3. Results

3.1 Protein structure prediction and modeling

The SWISS-MODEL online service was used to model the Cyp51A, MDR1, MDR2, MDR3, and MDR4 proteins. In addition, the crystallographic arrangement of Cyp51B (PDB code 5FRB) was obtained from the Protein Data Bank. The templates exhibiting high sequence coverage and Global Model Quality Estimation (GMQE) values were chosen. GMQE values usually range from 0 to 1,

with higher values indicating improved structural predictability (57). Multiple models were generated for each protein, and the model exhibiting the highest C-score was selected as the optimal candidate for subsequent analysis. Table 1**.** presented data on the 3-dimensional structures acquired and their respective levels of quality (Ramachandran, ERRAT, and VERIFY 3D). The Ramachandran plot is a graphical representation that illustrates the permissible and impermissible regions of protein residue backbone dihedral. A prerequisite for being deemed a high-quality model is over 85% of residues within permissible regions. ERRAT factor was another quality assessment. ERRAT is a non-bonded atomic interaction known as an overall quality factor, with more significant percentages indicating higher quality. Typically, the range for models of good quality exceeds 50. The total quality factor assessed for six proteins targets by the ERRAT server was within acceptable levels. Statistical data from the RC plot show that 90–94.1% of the residues in the modeled proteins belong to the most preferred region in the RC plot. This reveals that the modeled structures are accurate and reliable for further analysis. Findings from the ERRAT score also agree with the high accuracy of the modeled structures of the protein, where parameters range from 87.63 to 98.99%. The VERIFY 3D profile, which incorporates 3D and 1D features, necessitates a minimum of 80% of amino acids to possess a value exceeding 0.2. According to the projections made by the Verify 3D server, over 80% of the residues in the six proteins exhibited scores exceeding 0.2 (**Table 1**).

Table 1. Characterization and quality analysis of selected proteins for molecular docking with compounds selected

Protein Target	UniProt ID	METHOD	POSITIONS	ERRAT	VERIFY3D	Residues in most favored regions (Ramachandran)
Cyp51A	Q4WNT5	Swiss model	1-515	93.08%	87.04%	92.6%
Cyp51B	E9QY26	X-ray diffraction	50-518	87.63%	90.43%	90.0%
MDR1	Q4WTT9	Swiss model	1-1349	93.17%	83.37%	92.9%
MDR2	Q4WPP6	Swiss model	1-791	98.99%	80.17%	94.1%
MDR3	Q4WF45	Swiss model	1-528	94.37%	82.33%	93.3%
MDR4	Q4WSI1	Swiss model	1-1330	95.08%	80.94%	93.1%

3.2 Identification of physiochemical parameters

The physicochemical characteristics of six proteins were assessed through the ProtParam tool available on the ExPasy server. **Table 2.** presents the results of this analysis.

Table 2. The physicochemical properties of six designated proteins.

Parameter	Values					
	Cyp51A	Cyp51B	MDR1	MDR2	MDR3	MDR4
Molecular Weight (gm)	58068.0	58930.8	147784.4	85168.6	57042.2	144722.9
Number of Amino Acid	515	524	1349	791	528	1330
Theoretical PI	8.67	7.64	6.68	9.55	8.22	8.51
Aliphatic index	86.89	89.48	94.94	94.05	101.65	99.75
Instability index	42.96	43.95	33.93	36.09	49.09	39.54
GRAVY	-0.216	0.125	0.024	-0.038	0.430	0.107
Total number of negatively charged residues (Asp + Glu)	51	56	144	71	28	122
Total number of positively charged residues (Arg + Lys)	56	57	139	90	31	131

Proteins exhibiting an instability index below 40 are deemed stable, whereas those above 40 suggest potential instability. The calculated theoretical isoelectric point (pI) less than 7 indicates the acidic nature of the target protein, but the proteins with a pI higher than 7 indicate the alkaline nature. The aliphatic index of the target proteins indicates their thermal stability.

3.3. Molecular docking analysis

Affinity binding energy of compounds with thresholds as low as -8 for each protein target (Cyp51A, Cyp51B, MDR1, MDR2, MDR3, and MDR4) using the server (https://bioinformatics.psb.ugent) review and the Venn diagram was reported, which indicated that 20 compounds have the lowest affinity binding energy in the interaction of six proteins (**Fig. 2**). Docking Results of antifungal agents, similar structures as well as curcumin and its analogs with binding energy for each protein

target were reported in **Table 3** and **4.** The final score was determined by energy-minimizing poses and displayed as the docking score. The best-docked position with the lowest docking energy (better docking score) value was noted for each molecule. In the docking investigation, no limitations were utilized. After docking, top-ranked molecules were sorted based on their docking score. The positive binding is indicated by the decrease in docking energy (better docking score).

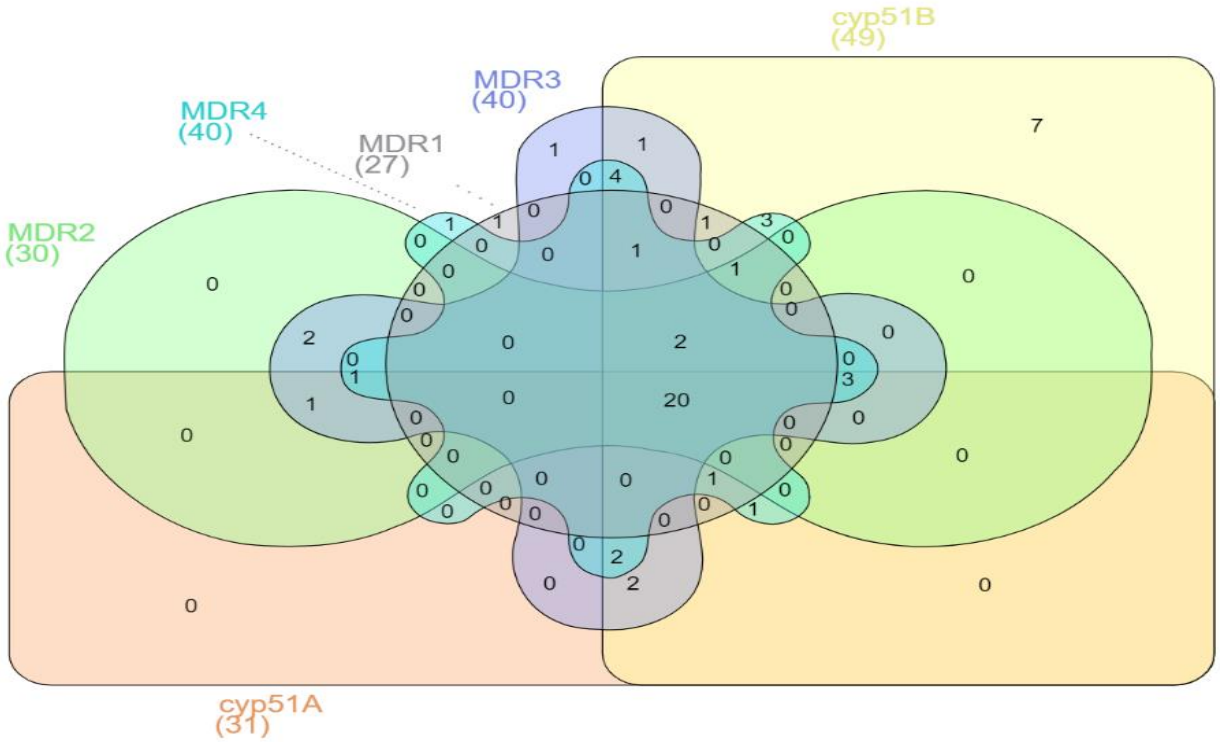

Fig. 2. Intersection of 20 compounds with the lowest binding energy on six protein targets

Table 3. Docking Results of antifungal agents and similar structures with the lowest binding energy.

Compounds name	Binding Energy(kcal/mol)						PubChem CID
	Cyp51A	Cyp51B	MDR1	MDR2	MDR3	MDR4	
Pramiconazole	-11.5	-12.1	-9.7	-10.4	-10.8	-10.2	3013050
Saperconazole	-11.5	-11.7	-9.5	-9.5	-10.7	-9.6	9809993
Itraconazole	-11	-9.3	-8.8	-8.9	-10.5	-9.8	55283
Oteseconazole	-9.4	-11.9	-9	-8.8	-9.6	-9.5	77050711
Olorofim	-10.7	-9	-9.1	-9.2	-10.4	-8.9	91885568
Quilseconazole	-9.8	-9.1	-9.5	-9	-10.5	-9.2	91886002
Amphotericin B	-9.7	-8.9	-8.4	-9.9	-9.7	-10.2	5280965
Nystatin	-10.9	-8.9	-8.7	-8.8	-10.4	-8.7	6433272
35-Deoxyamphotericin B	-9.6	-8.2	-8.6	-8.8	-11.2	-9.9	101481774
Ketoconazole N-Oxide	-9.9	-9.5	-8.8	-8.6	-9.1	-9.1	129318412
2,3-Dehydro Ketoconazole	-9.6	-9.1	-9.1	-8.5	-9.6	-9	71315319
Methylamphotericin B	-8.8	-8.6	-8.7	-9.5	-10.2	-9	11968030
ketoconazole	-9.1	-10	-8.7	-8.7	-9.4	-8.8	456201
Voriconazole	-8.5	-8.4	-8.5	8.7	-8.3	-8.6	11968030
Triaconazole	-9.1	-8.8	-8.5	-8.1	-8.6	-8.9	441383
Nikkomycin	-8.3	-8.6	-9	-8.4	-8.8	-8.5	456557
Dichlorophenyl Imidazoldioxolan (Elubiol)	-8.9	-8.7	-8	-8.1	-8.7	-9	158496
Efinaconazole	-8.2	-8.1	-8.7	-8.4	-8.9	-8.7	489181
Voriconazole N-Oxide	-8.6	-8.4	-8.1	-8.2	-8.4	-8.5	10044355
Fluconazole	-8.1	-8.7	-8.3	-8.4	-8	-8.1	3365

Table 4. The binding energy of curcumin and its analogs in interaction with six critical genes related to *Aspergillus* drug resistance.

Compounds name	Binding Energy						PubChem CID
	Cyp51A	Cyp51B	MDR1	MDR2	MDR3	MDR4	
Difluorinated curcumin(CDF)	-9.7	-9.6	-9.7	-8.7	-9.3	-10.2	54597187
Cyclocurcumin	-8.6	-8.7	-8.7	-8.2	-8.9	-9.9	69879809
Curcumin	-8.3	-9.2	-8.6	-8	-8.3	-8.9	969516
Curcumin sulfate	-8.6	-8.6	-7.6	-7.5	-7.8	-8.5	66645351
Dimethoxycurcumin	-8	-8	-7.7	-7	-8.2	-7.6	9952605
Tetrahydrocurcumin	-7.4	-7.7	-7.5	-7	-8.1	-8.4	56965746

The analyzing H-bonds of the lowest affinity binding energy and their distance compared to curcumin and its analogs were reported in **Table 5**. The molecular binding analysis illustrated the H-bonding interaction of pramiconazole (with the lowest binding energy), curcumin (as a candidate natural compound in the current study), and CDF (as a curcumin analog with the lowest binding energy) between protein targets in **Figs. 3, 4, and 5.**

Table 5. The details of the H-bond of 3 candidate ligands in interaction with six target proteins

Drug-protein interaction	H-bond	Donor Atom	Acceptor Atom	Distance
Pramiconazole –Cyp51A	N:UNK1:HN - A:SER486:OXT	HN	OXT	2.37921
Pramiconazole –Cyp51B	A: ILE232: HN - N: UNK1: O	HN	O	2.35471
	A: GLN309:HE22 - N: UNK1: O	HE22	O	2.49528
Pramiconazole –MDR1	N:UNK1:HN- A:GLN952:OE1	HN	OE1	2.3318
	A:ASN396:HD21 - N:UNK1:F	HD21	F	2.46315
Pramiconazole –MDR2	N: UNK1: HN - B: ARG251: O	HN	O	2.4633
Pramiconazole –MDR3	N: UNK1: HN - A: ARG321: O	HN	O	2.14335
	N: UNK1: HN - A: LEU69: O	HN	O	1.85045
	A: HIS73:HE2 - N: UNK1: O	HE2	O	2.42012
Pramiconazole –MDR4	N: UNK1: HN - A: LEU917: O	HN	O	2.2662
	A: GLN382:HE21 - N: UNK1: O	HE21	O	2.40393
Curcumin– Cyp51A	N: UNK1: H - A: GLY448: O	H	O	2.34549
Curcumin– Cyp51B	A: ASN427:HD21 - N: UNK1: O	HD21	O	2.39427
	A: ARG462:HH11 - N: UNK1: O	HH11	O	1.89431
	A: ARG462:HH21 - N: UNK1: O	HH21	O	2.40787
Curcumin– MDR1	N:UNK1:H - A:GLU851:OE1	H	OE1	1.95859
	N:UNK1:H - A:GLU851:OE2	H	OE2	2.46857
	A: SER14: HG - N: UNK1: O	HG	O	2.49722
	A: LYS1069:HZ2 - N: UNK1: O	HZ2	O	2.48335
Curcumin– MDR2	N: UNK1: H - B: LEU236: O	H	O	2.13029
	N:UNK1:H - B:SER192:OG	H	OG	2.29926
	N: UNK1: H - B: TYR454: O	H	O	2.46342
	A: ASN421:HD21 - N: UNK1: O	HD21	O	2.22288
Curcumin– MDR3	N: UNK1: H - A: TRP310: O	H	O	2.17328
	N: UNK1: H - A: ALA498: O	H	O	2.12728
	A: CYS382: HG - N: UNK1: O	HG	O	2.46257
Curcumin– MDR4	N:UNK1:H - A:ASN339:OD1	H	OD1	2.49692
	A: ASN339:HD21 - N: UNK1: O	HD21	O	1.95931
	A: GLN1035:HE21 - N: UNK1: O	HE21	O	2.30315
CDF-Cyp51A	N: UNK1: H - A: PHE208: O	H	O	2.48255
CDF-Cyp51B	A: ASN427:HD21 - N: UNK1: O	HD21	O	2.0293
	A: ARG462:HH11 - N: UNK1: O	HH11	O	1.77081
	A: ARG462:HH21 - N: UNK1: O	HH21	O	2.26684
CDF-MDR1	N: UNK1: H - A: ASN392: O	H	O	1.86105
	A:ASN392:HD22 - N:UNK1:F	HD22	F	2.44011
	A: ASN396:HD21 - N: UNK1: O	HD21	O	2.11617
	A: GLN1015:HE21 - N: UNK1: O	HE21	O	2.23157
CDF-MDR2	N:UNK1:H - A:ASP278:OD1	H	OD1	2.42228
	A: ARG579:HH11 - N: UNK1: O	HH11	O	2.35949
	A: ARG579:HH21 - N: UNK1: O	HH21	O	2.45294
CDF-MDR3	A: GLN150:HE22 - N: UNK1: O	HE22	O	2.36326
CDF-MDR4	A: SER998: HG - N: UNK1: O	HG	O	2.25399

UNK: compound or drug, GLY: Glycine, VAL: Valine, LEU: Leucine, MET: Methionine, SER: Serine, ARG: Arginine, GLU: Glutamic acid, LYS: Lysine, ALA: Alanine, ASP: Aspartic acid, ASN: Asparagine, THR: Threonine, GLN: Glutamine, HIS: Histidine, H: Hydrogen, O: Oxygen, N: Nitrogen

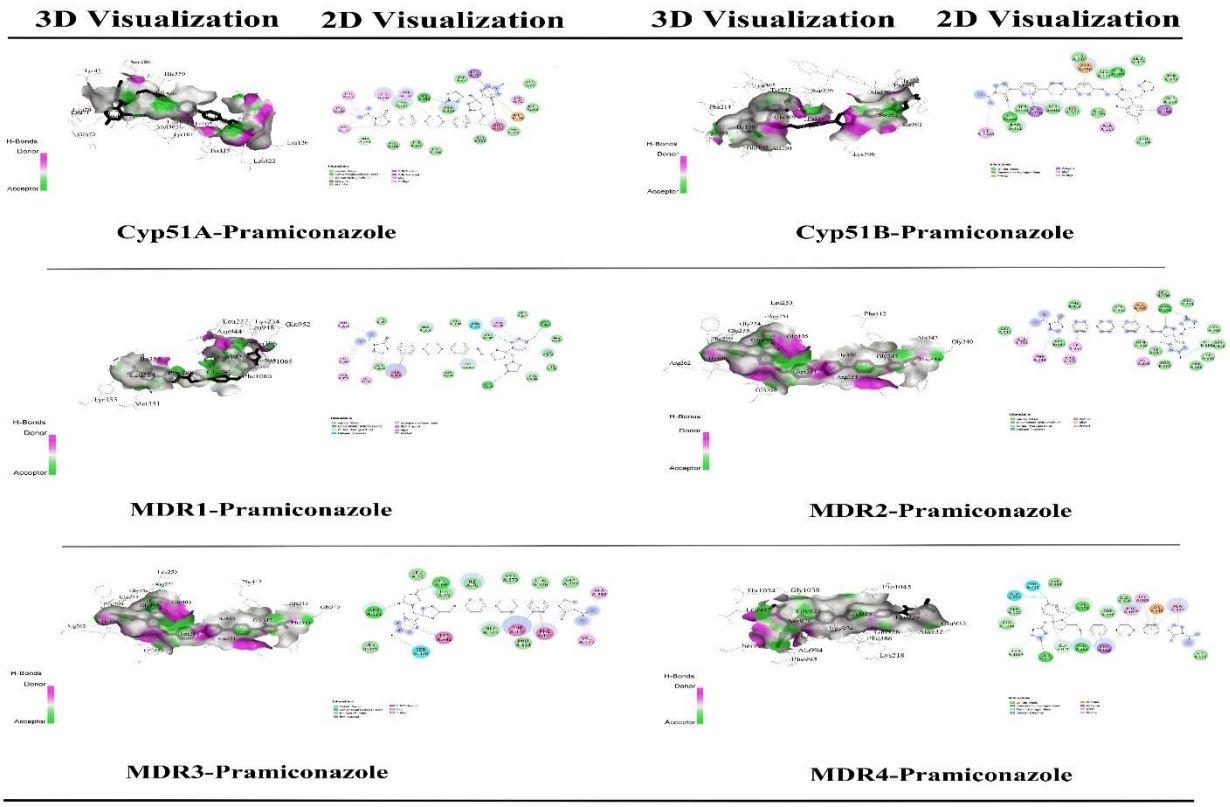

Fig. 3. The 3D and 2D visualization of docking analysis of pramiconazole molecular interaction with six target proteins.

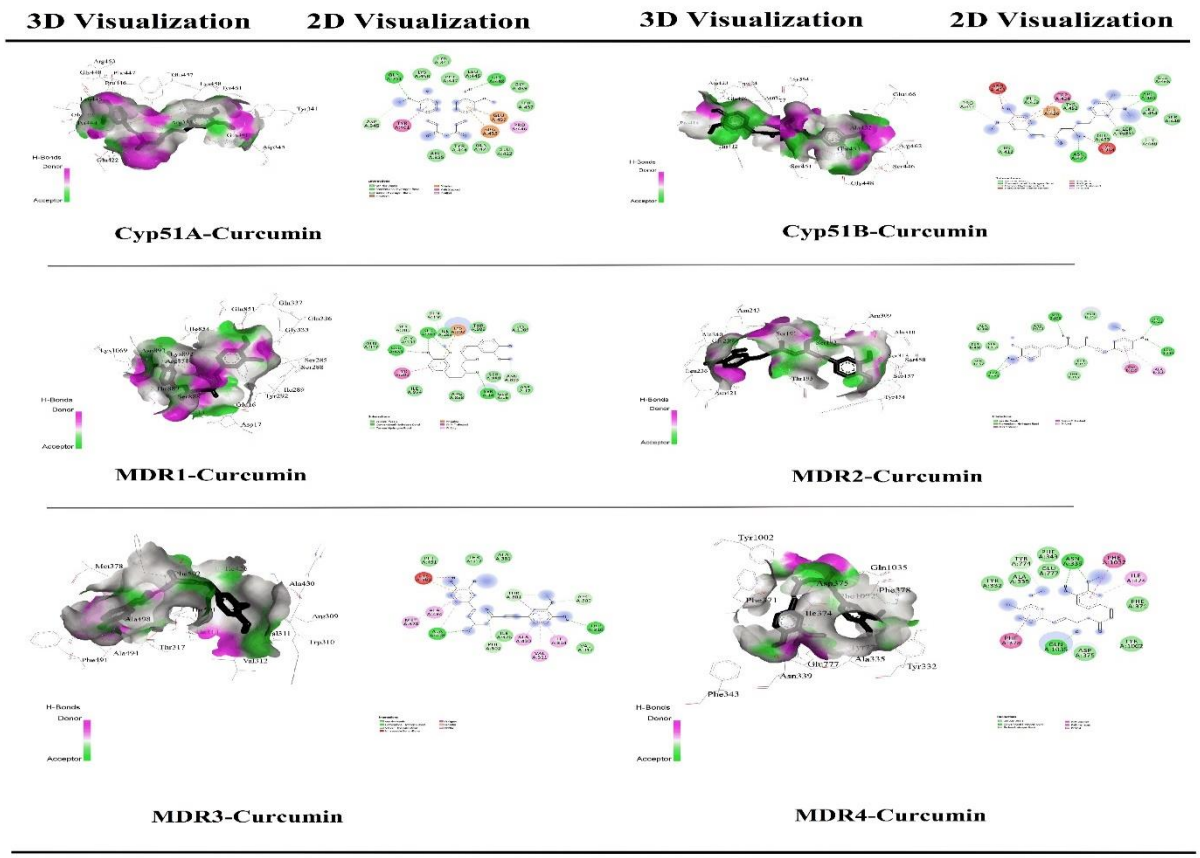

Fig. 4. The 3D and 2D visualization of docking analysis of curcumin molecular interaction with six target proteins.

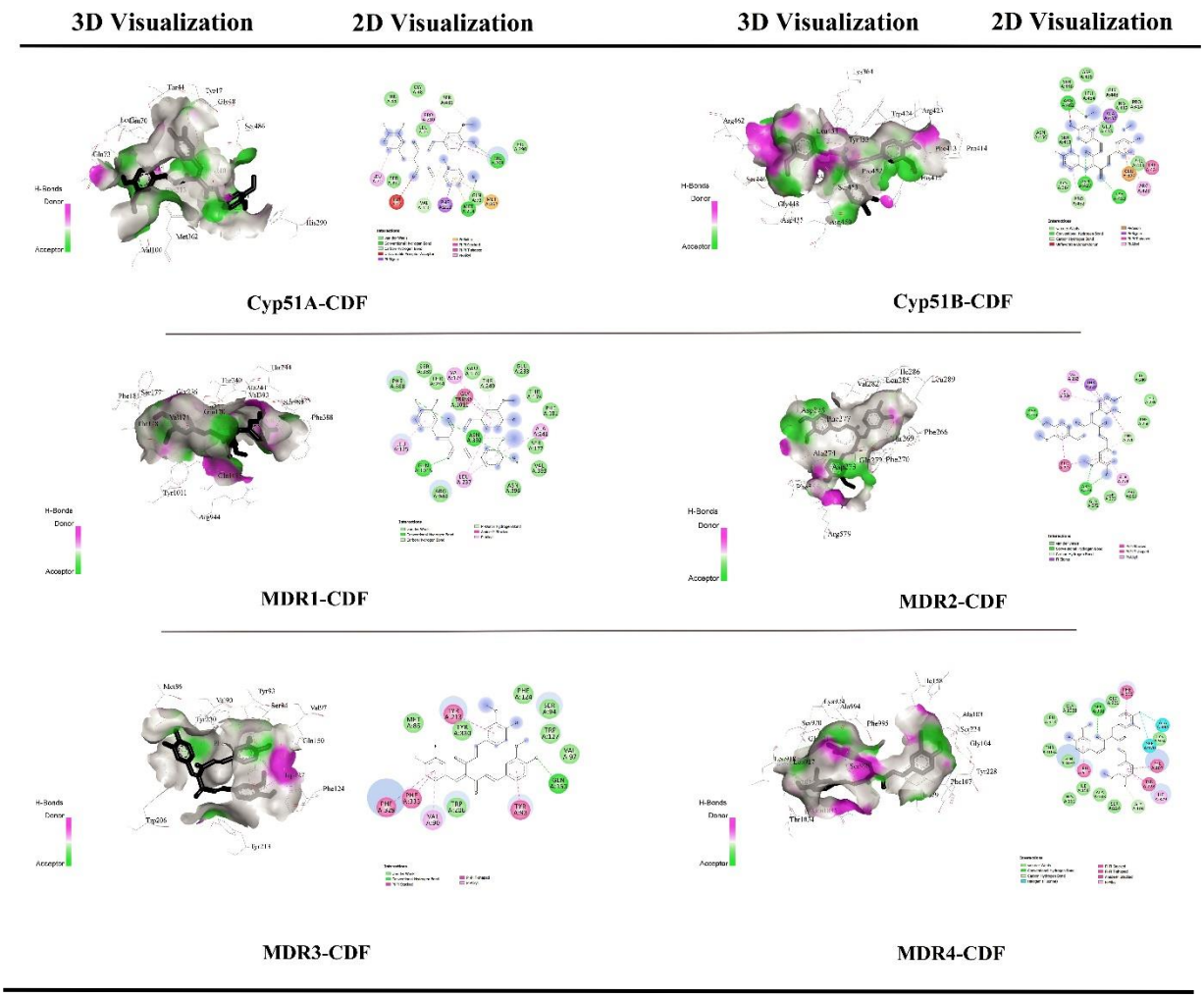

Fig. 5. The 3D and 2D visualization of docking analysis of CDF molecular interaction with six target proteins.

3.3 Prediction of ADME and drug-likeness

The ADME screening and drug-likeness evaluation were performed by inserting canonical SMILES into the Swiss-ADME server.

3.3.1 Swiss-ADME selectivity factors for top compounds

Several ADME features of the top 10 compounds, curcumin, and its analogs, including water-solubility, Bioavailability Score, BBB Permeant, and GI Absorption, are provided to evaluate the potential for drug ability (**Table 6**). They were calculated by using the SwissADME Online server. Pramiconazole, saperconazole, itraconazole, oteseconazole, olorofim, quilseconazole, and ketoconazole N-Oxide had the poorest solubility. Amphotericin B, nystatin, and 35-deoxyamphotericin B are soluble. Curcumin and its analogs, except CDF, were found to be moderately soluble, while that CDF has poor solubility. Within the category, 30% of the compounds exhibited elevated bioavailability scores. Also, curcumin and its analogs showed high bioavailability scores. All compounds except oteseconazole, quilseconazole, amphotericin B, nystatin, 35-deoxyamphotericin B, and curcumin sulfate exhibited a high GI absorption.

Table 6. Swiss-ADME analysis of top 10 compounds, curcumin, and its analogs docked against six target proteins.

Compounds	Water Solubility	Bioavailability Score	BBB Permeant	GI Absorption
Pramiconazole	Poor	0.17	No	High
Saperconazole	Poor	0.17	No	High
Itraconazole	Poor	0.17	No	High
Oteseconazole	Poor	0.17	No	Low
Olorofim	Poor	0.55	No	High
Quilseconazole	Poor	0.55	No	Low
Amphotericin B	Soluble	0.17	No	Low
Nystatin	Soluble	0.17	No	Low
35-Deoxyamphotericin B	Soluble	0.17	No	Low
Ketoconazole N-Oxide	Poor	0.55	No	High
Curcumin and its analogs				
Curcumin	Moderate	0.55	No	High
CDF	Poor	0.55	No	High
Cyclocurcumin	Moderate	0.56	No	High
Curcumin sulfate	Moderate	0.56	No	Low
Dimethoxycurcumin	Moderate	0.55	Yes	High
Tetrahydrocurcumin	Moderate	0.55	No	High

3.3.2. Investigation of drug-likeness

The compounds' drug-likeness was assessed based on Lipinski's rule of five characteristics. The initial parameter pertains to the maximum allowable molecular weight threshold, with a value of 500 or less. The molecular weight of the olorofim, curcumin, and its analogs is lower than 500 g/mol, but other compounds (All of the top 10) did not follow this rule. The second parameter restricts H-band acceptors to a maximum of 10 (HBA ≤ 10), while the third parameter restricts H-band donors to a maximum of 5 (HBD ≤ 5). The last parameter sets a threshold for the consensus log p-value at a maximum of 5 (log p ≤ 5). In **Table 7**, the drug-likeness of all compounds is shown. The consensus log P values for amphotericin B and nystatin are negative, indicating that these compounds have a greater affinity for the aqueous phase. Compounds such as pramiconazole, curcumin, and its analogs adhere to all five rules but do not assure drug-likeness. Nonetheless, they are more likely to demonstrate improved absorption through the oral route. Also, the inadequacy of these parameters does not necessarily mean the complete loss of drug effectiveness. Moreover, passing these parameters does not necessarily indicate the oral activity of the compounds. According to the previous cases, additional features regarding drug similarity were considered, including a topological polar surface area (TPSA) not exceeding 140 and the number of rotatable bonds (RB) not exceeding 10, as these factors could offer more precise estimations concerning oral bioavailability.

Table 7. Lipinski of parameters to examine drug-likeness of top 10 compounds, curcumin, and its analogs

Compounds	Mol. Weight (g/mol)	Rotatable Bonds	H Bond Acceptors	H Bond Donors	TPSA	C Log *p*
	MW ≤ 500	**RB ≤ 10**	**HBD ≤ 10**	**HBA ≤ 5**	**(Å^2) ≤ 140**	**Log *p* ≤ 5**
Pramiconazole	659.73	10	8	0	88.43	4.06
Saperconazole	672.72	11	9	0	104.70	4.28
Itraconazole	705.63	11	7	0	104.70	4.71
Oteseconazole	527.39	9	13	1	85.95	4.79
Olorofim	498.55	7	5	1	83.36	3.45
Quilseconazole	513.37	8	13	1	85.95	4.76
Amphotericin B	924.08	3	18	12	319.61	-0.39
Nystatin	926.09	3	18	12	319.61	-0.18
35-Deoxyamphotericin B	908.08	3	17	11	299.38	0.27
Ketoconazole N-Oxide	547.43	8	7	0	95.26	2.16
Curcumin and its analogs						
Curcumin	368.38	8	6	2	93.06	3.03
CDF	492.47	9	8	2	93.06	4.99
Cyclocurcumin	368.38	5	6	2	85.22	2.82
Curcumin sulfate	448.44	10	9	2	144.81	2.42
Dimethoxycurcumin	396.43	10	6	0	71.06	3.65
Tetrahydrocurcumin	372.41	10	6	2	93.06	3.05

3.4. Toxicity prediction

Toxicity is an essential factor in selecting the best drug compounds. The toxicity of the compounds was evaluated using the online machine-learning tools ProTox-II, PkCSM, and StopTox. The ProTox-II system employs a classification scheme consisting of six distinct toxicity classes (ranging from 1 to 6) determined dependent on the LD50 value. This classification system is found on a globally harmonized chemical classification and labeling system called GHS. The classification of LD50 values is as follows: Class 1: Fatal if ingested (LD50 ≤ 5). Class 2: in case of lethal consumption (5 < LD50 ≤ 50). Class 3: Dangerous if swallowed (50 < LD50 ≤ 300). Amphotericin B, nystatin, and 35-deoxyamphotericin B were in class 3, indicating possible toxicity risks upon oral exposure. The fourth class of compounds on the list has a toxicity rating ranging from 300 to 2000 LD50 units and is considered hazardous if consumed. This category contains ten of the total sixteen compounds listed. Pramiconazole and curcumin are members of this group. Four of the compounds on the list fall into the fifth class and could be dangerous if ingested (2000 < LD50 ≤ 5000). The sixth classification (LD50 > 5000) contains only non-toxic substances. In this study, no compounds belonging to class 6 were identified. In addition, using the pkCSM server, three critical parameters, including hepatotoxicity potential, maximum tolerated dose in humans, and AMES toxicity, were investigated. Among the 16 compounds in the table below, eight are not hepatotoxicity. The preferred range for the maximum tolerated dose of a compound in humans for probable drug candidates should be ≤ 0.477 log (mg/kg/day). Hence, seven compounds have been demonstrated to be well tolerated by humans. Humans can tolerate C curcumin and CDF according to the declared permissible limit with a dose value of 0.081 and 0.075, respectively, while pramiconazole, with a dose value of 0.905, is not within the acceptable range for humans (58). AMES toxicity is used to forecast drug compound carcinogenicity. None of the compounds demonstrated AMES toxicity **(Table 8).**

Table 8. Toxicity prediction reported of critical compounds using ProTox-II and pkCSM servers (Top10 Compound, curcumin and its analogs)

ProTox-II			pkCSM		
Compounds	**LD50 Value (mg/kg)**	**Toxicity Class**	**Hepatotoxicity**	**Max. tolerated dose (human) (log mg/kg/day)**	**AMES toxicity**
Pramiconazole	320	4	Yes	0.905	No
Saperconazole	4000	5	Yes	0.879	No
Itraconazole	320	4	Yes	0.91	No
Oteseconazole	1000	4	Yes	0.523	No
Olorofim	1420	4	Yes	0.62	No
Quilseconazole	450	4	Yes	0.503	No
Amphotericin B	100	3	No	0.292	No
Nystatin	100	3	No	0.281	No
35-Deoxyamphotericin B	100	3	No	0.279	No
Ketoconazole N-Oxide	1000	4	Yes	0.956	No
Curcumin and its analogs					
Curcumin	2000	4	No	0.081	No
CDF	4000	5	Yes	0.075	No
Cyclocurcumin	1500	4	No	0.046	No
Curcumin sulfate	4000	5	No	0.689	No
Dimethoxycurcumin	2000	4	No	0.671	No
Tetrahydrocurcumin	2580	5	No	0.125	No

STopTox is an extensive assemblage of computational models that can forecast chemical toxicity hazards as a substitute for in vivo experiments. The purpose of this analysis was to determine if exposure to the compounds could result in a type of acute toxicity. None of the compounds examined in this study demonstrated indications of acute inhalation toxicity, except CDF, cyclocurcumin, and Curcumin sulfate. Six of the sixteen compounds proved positive for acute oral toxicity. Pramiconazole was also one of the compounds with acute oral toxicity. Only cyclocurcumin was determined to be positive for dermal toxicity among all compounds examined. Four compounds, including oteseconazole, curcumin, curcumin sulfate, and CDF, had positive skin sensitivity. Most compounds cause eye irritation and corrosion except for curcumin and its analogs. Also, it was demonstrated that no compounds cause skin irritation and corrosion **(Table 9).**

Table 9. Acute toxicity analysis was carried out using the StopTox server for top compounds.

Compounds	StopTox Acute Toxicity Analysis					
	Acute Inhalation Toxicity	Acute Oral Toxicity	Acute Dermal Toxicity	Eye Irritation and Corrosion	Skin Sensitization	Skin Irritation and Corrosion
Pramiconazole	No	Yes	No	Yes	No	No
Saperconazole	No	Yes	No	Yes	No	No
Itraconazole	No	Yes	No	Yes	No	No
Oteseconazole	No	Yes	No	Yes	Yes	No
Olorofim	No	Yes	No	Yes	No	No
Quilseconazole	No	No	No	Yes	No	No
Amphotericin B	No	No	No	Yes	No	No
Nystatin	No	No	No	Yes	No	No
35-Deoxyamphotericin B	No	No	No	Yes	No	No
Ketoconazole N-Oxide	No	Yes	No	Yes	No	No
Curcumin and its analogs						
Curcumin	No	No	No	No	Yes	No
CDF	Yes	No	No	No	Yes	No
Cyclocurcumin	Yes	No	Yes	No	No	No
Curcumin sulfate	Yes	No	No	No	Yes	No
Dimethoxycurcumin	No	No	No	No	No	No
Tetrahydrocurcumin	No	No	No	No	No	No

3.5 PASS Online Predictions

The PASS programs' predictions are based on examining the correlation between structure and activity within a heterogeneous training dataset encompassing pharmaceutical agents, drug compounds, and drug candidates at different phases of clinical and preclinical investigation. The values of Pa and Pi exhibit variation within the range of 0.000 to 1.000. It is generally observed that the summation of Pa and Pi should not be equal to one. If the Pa value exceeds 0.70, the compound will exhibit the desired experimental activity. **Table 10** lists compounds exhibiting bioactivities that either meet or surpass a Pa value of 0.7. Compounds can be classified into three categories based on their bioactivity scores. A score greater than 0.0 is considered "active," while a score between 5.0 and 0.0 is considered "moderately active." Compounds with a bioactivity score of -5.0 are classified as "inactive." These classifications suggest that with some chemical structure modifications, the compounds may have the potential as drugs.

Table 10. The biological activity and predicted bioactivity outcomes for the selected compounds.

Compounds	Biology activity (pa > 0.7)	Molinspiration					
		GPCR ligand	Ion channel modulator	Kinase inhibitor	Nuclear receptor ligand	Protease inhibitor	Enzyme inhibitor
Pramiconazole	Antifungal activity	-0.20	-1.06	-0.74	-1.01	-0.15	-0.69
Saperconazole	Lanosterol 14 alpha demethylase inhibitor, Antifungal, CYP51 inhibitor	-0.41	-1.50	-1.24	-1.27	-0.61	-0.96
Itraconazole	Lanosterol 14 alpha demethylase inhibitor, Antifungal, CYP17 inhibitor, CYP51 inhibitor	-0.40	-1.50	-1.30	-1.31	-0.66	-0.97
Oteseconazole	CYP2C19 inhibitor	0.25	-0.14	-0.09	0.15	0.30	0.10
Olorofim	Platelet derived growth factor receptor kinase inhibitor	0.11	-0.22	0.23	-0.27	-0.26	-0.01
Quilseconazole	Cytochrome P450 inhibitor	0.32	0.00	0.11	0.19	0.38	0.11
Amphotericin B	Antiprotozoal (Leishmania and Amoeba), Anti-infective, Antifungal, Antibacterial	-3.06	-3.51	-3.54	-3.45	-2.45	-2.95
Nystatin	Antiprotozoal (Amoeba), Anti-infective, Antifungal, Antiprotozoal (Leishmania), Antibacterial	-3.04	-3.51	-3.54	-3.44	-2.45	-2.93
35-Deoxy Amphotericin B	Antiprotozoal (Leishmania, Amoeba), Anti-infective, Membrane integrity antagonist Antifungal, Antibacterial	-2.93	-3.41	-3.49	-3.42	-2.27	-2.85
Ketoconazole N-Oxide	27-Hydroxycholestrol 7alpha-monooxygenase inhibitor, CYP17,51 inhibitor, Lanosterol 14 alpha demethylase inhibitor	0.27	-0.18	-0.20	-0.31	-0.20	0.23
Curcumin and its analogs							
Curcumin	Feruloyl esterase inhibitor, Membrane integrity agonist, Monophenol monooxygenase inhibitor, Reductant	-0.06	-0.20	-0.26	0.12	-0.14	0.08
CDF	JAK2 expression inhibitor, Feruloyl esterase inhibitor, Prostate cancer treatment, HIF1A expression inhibitor	-0.10	-0.26	-0.18	-0.05	-0.14	-0.03
Cyclocurcumin	Feruloyl esterase inhibitor, Free radical scavenger, JAK2 expression inhibitor, *CYP51A* inhibitor	-0.04	-0.31	-0.28	0.10	-0.11	0.09
Curcumin sulfate	Glutathione S-transferase substrate, HIF1A expression inhibitor, Monophenol monooxygenase inhibitor JAK2 expression inhibitor, CYP2C12 substrate	0.13	-0.23	-0.27	0.04	0.22	0.44

Dimethoxycurcumin	HIF1A expression inhibitor, JAK2 expression inhibitor, Feruloyl esterase inhibitor, MMP9 expression inhibitor, Apoptosis agonist	-0.09	-0.23	-0.28	0.04	-0.14	0.02
Tetrahydrocurcumin	HIF1A expression inhibitor, 5Hydroxytryptamine release stimulant, JAK2 expression inhibitor, MMP9 expression inhibitor	0.05	-0.04	-0.23	0.12	0.00	0.13

4. Discussion

Aspergillosis is a group of non-contagious, opportunistic, and different mycoses caused by species of *Aspergillus* (59). Few *Aspergillus* species cause serious infections, but individuals with transplants, those taking immunosuppressive medications, or those with AIDS, diabetes, or blood cancers are more likely to develop aspergillosis. It can also occur in immunocompetent patients. *A. fumigatus* is the most prevalent species of *Aspergillus* that causes invasive clinical forms (60). Azoles are commonly employed for the treatment of aspergillosis. These antifungal agents function by inhibiting the 14-sterol demethylase (14-DM, CYP51), a monooxygenase in fungal cells that plays a crucial role in biosynthesis of ergosterol (61). Cyp51 is the gene that encodes both the Cyp51A and Cyp51B enzymes, which are azole drug targets required for ergosterol production, which is required for various fungal metabolic functions, including membrane integrity and permeability, cell cycle progression, and cell shape. As a result, specific inhibition of these enzymes is critical for ensuring an appropriate therapeutic response (62). Previous studies determined that azole antifungals work by directly inhibiting the Cyp51 proteins, which results in the gradual creation of carbohydrate regions in the cell wall and the accumulation of toxic sterol intermediates within the cell the loss of ergosterol in the cell membrane (63). Treatment-resistant *Aspergillus* species to triazoles have been linked to point changes in Cyp51A, tandem repeats in the promoter of Cyp51A, and upregulation of Cyp51A (64). Reported elevated constitutive and azole-inducible Cyp51B expression levels in two clinical isolates resistant to azoles despite having wild-type Cyp51A. The statement suggests a possible link between azole resistance and Cyp51B (65). It was also shown that Cyp51B's heme group is crucial to the synthesis of the cell wall of *A. fumigatus*. The heme group, encoded in a strategically important position within the active region of CYP51B, is an essential component of this protein. Therefore, eliminating this section could prevent this protein from functioning in fungal cell wall formation (66). The overexpression of efflux transporters MDR1-4 in clinical isolates impedes the accumulation of triazoles through their extrusion from the cell, ultimately leading to the development of resistance (67). Studies have demonstrated that the upregulation of efflux transporters can enhance the drug resistance of *Aspergillus* (68, 69). Pramiconazole is a newly developed triazole antifungal agent that functions by impeding the synthesis of ergosterol in fungal cell membranes. It leads to augmented cell permeability and destruction and exhibits robust in vitro anti-dermatophyte and anti-yeast activities akin to existing antifungal medications (70). In preclinical investigations, pramiconazole demonstrated antifungal activity comparable to or superior to itraconazole and ketoconazole. It was found to have a wide range of activities inhibiting ergosterol synthesis (71). Another study found that oral and topical pramiconazole formulations were more efficient than itraconazole and terbinafine in inhibiting *Microsporum canis* formation in guinea pigs (72). According to the molecular docking data in this study, pramiconazole, as a multi-target ligand, had the lowest binding energy with all six target proteins compared to other selective ligands. The drug-likeness evaluation of pramiconazole indicated that all parameters except molecular weight met Lipinski's guidelines. It has low solubility and high GI absorption. The results of the toxicity evaluation using the ProTox-II server specified that this compound has a toxicity class of 4 and an LD50 of 320 mg/kg. pkCSM analysis indicated that pramiconazole is hepatotoxic. StopTox outcomes determined that this compound does not result in acute oral toxicity, eye irritation, or corrosion. It may be toxic in cases of acute inhalation or dermal toxicity. Based on bioactivity prediction with PASS online server, this compound inhibits aldosterone 14 alpha demethylase and can be considered an antifungal agent. Plant-derived natural compounds were demonstrated to block the development of the fungal cell wall, sphingolipids, and protein, making them attractive antifungal agents. Curcumin, a compound derived from plants, has been the subject of extensive research and is reported to possess antifungal activity (73-75). The study revealed

that curcumin exhibited antifungal properties against *Candida albicans* and modulated proteolytic enzyme activities without significantly impacting gene expression (76). Curcumin also has biological effects on *C. albicans*, notably stopping biofilm formation and affecting how the cells stick together (77). Researchers have also determined that combining fungicide products, curcumin, and photodynamic therapy might synergistically enhance the efficacy of existing antifungal strategies (78, 79). In this study, curcumin displayed binding affinity -8.3 and -9.2 kcal/mol with Cyp51A and Cyp51B, respectively. In addition, docking data indicate that the interaction between curcumin and MDR1-4 has a considerable binding affinity. According to the Swiss-ADME evaluation, its solubility is moderate, its GI absorption is high, and its bioavailability score is 0.55. The molecule has a molecular weight of 368.38 g/mol, six H-bond acceptors, and two H-bond donors, and drug-likeness assessment shows that curcumin does not violate Lipinski's principles. As a result, it has the potential to become a medication. Furthermore, pkCSM analysis suggests that curcumin is not hepatotoxic. Based on ProTox-II, this compound has a toxicity class of 4 and an LD50 of 4000 mg/kg. By StopTox server analysis, curcumin may not induce acute inhalation, cutaneous, or oral toxicity. However, it can cause skin sensitivity. Curcumin has active bioactivity ratings in nuclear receptor ligand and enzyme inhibitor, and average bioactivity scores in GPCR ligand, ion channel modulation, kinase inhibition, and protease inhibition, according to the results of the web-based tool Molinspiration. In the present research, CDF with the lowest binding energy against gene overexpression produces the 14-a-sterol demethylase enzyme (Cyp51A and Cyp51B) and resistance by multidrug efflux pumps (MDR1-4) in *Aspergillus* spp. can be considered a promising candidate for use as an antifungal agent. CDF is a new and efficient fluorinated curcumin analog more bioavailable than curcumin. It has been revealed to inhibit growth more effectively than curcumin (80). Prior research has established that curcumin analogs exhibit enhanced synergistic antifungal efficacy against *Candida* species resistant to fluconazole, demonstrating promising prospects for developing novel anti-drug-resistant fungal therapeutics (81). In recent years, medicinal chemists worldwide have made massive efforts to generate structurally modified, therapeutically useful curcumin analogs/derivatives. Dong *et al*. conducted a study that employed curcumin derivatives to recover fluconazole potency against *Candida* species resistant to fluconazole. These compounds displayed suitable antifungal activities (82). Regarding the antifungal effects of CDF, Zarrinfar *et al.* observed that both CDF and curcumin suppressed the growth of dermatophytic strains under *in vitro*. CDF outperformed curcumin, particularly against *Trichophyton interdigitale*. CDF and curcumin have the potential to be developed for use in dermatophytosis to supplement existing treatments (83). Based on the findings of this research, this compound exhibited favorable interactions in docking studies against all the targets compared to other curcumin analogs. The compound CDF exhibits a molecular weight of 492.47 g/mol and possesses 8 H-bond acceptors as well as 2 H-bond donors. Furthermore, it satisfies all of the Lipinski parameters. The ADME profile of the compound indicated reduced aqueous solubility, elevated absorption in the gastrointestinal tract, and a bioavailability index of 0.55. Toxicity studies assigned an LD50 of 4000 mg/kg to this compound, placing it in toxicity class 5, and a pkCSM analysis indicated that CDF is hepatotoxic. Furthermore, the results obtained from StopTox indicate a favorable toxicity profile, with no acute inhalation, dermal, oral, cutaneous, or ocular toxicity, or skin corrosion. Predictions of its bioactivity indicate that it could be a JAK2 expression inhibitor, a feruloyl esterase inhibitor, or a HIF1A expression inhibitor. Also, the result of the Molinspiration server has shown that it can act as a kinase, protease, and enzyme inhibitor. In this work, after thoroughly screening all known ligands, pramiconazole, and CDF were the most effective inhibitors of Cyp51A, and Cyp51B, compared to curcumin and another selected compound and MDR-1–4. There is the possibility that these compounds might not perform better in all screening tests. In addition, the results of this investigation indicate that their potential toxicity is limited. Due to the computational nature of this research, *in vitro* and *in vivo* analyses are recommended to determine these compounds' target inhibition potential accurately.

5. Conclusions

Through *in silico* prediction and molecular docking, this study has identified potential compounds for treating *Aspergillus* infections. Among the compounds assessed, pramiconazole, CDF, and curcumin demonstrated higher binding affinity with six crucial proteins, indicating their potential as effective agents against *Aspergillus* species. However, further optimization is necessary to address unfavorable parameters for predicting toxicity and ADME before these compounds can be considered for human consumption. Despite the need for optimization, toxicity analysis suggests that the compounds have a favorable toxicity profile. Furthermore, no toxicity was observed through inhalation, dermal, oral, cutaneous, or ocular exposure, and no skin corrosion according to ProTox-II, pkCSM and StopTox servers. While these findings were derived from *in silico* research, they hold promising implications for developing effective treatments for *Aspergillus* infections. To validate the results and explore the clinical potential of these compounds, we recommend conducting *in vitro* and *in vivo* experiments. By combining *in silico* analysis with *in vitro* and *in vivo* investigations, new treatments against *Aspergillus* species could be developed.

Declarations

Acknowledgement
Not applicable.

Availability of data and materials
Available data are presented in the manuscript.

Ethical approval and consent to participate
Not applicable.

Funding
This research received no external funding.

Author Contributions
Conceptualization, M.J.J-N.; methodology, M.J.J-N., software, M.J.J-N., formal analysis, M.J.J-N.; investigation, M.J.J-N.; data curation, M.J.J-N; writing—original draft preparation, M.J.J-N. and T.A; writing—review and editing, M.J.J-N. and H.Z.; supervision, H.Z.; All authors have read and agreed to the published version of the manuscript.

Consent for publication
Not applicable.

Competing interests
The authors declare that they have no competing interests.

References

1. Zanganeh E, Zarrinfar H, Rezaeetalab F, Fata A, Tohidi M, Najafzadeh MJ, et al. Predominance of non-fumigatus Aspergillus species among patients suspected to pulmonary aspergillosis in a tropical and subtropical region of the Middle East. Microbial pathogenesis. 2018;116:296-300.
2. Najafzadeh MJ, Dolatabadi S, Zarrinfar H, Houbraken J. Molecular diversity of aspergilli in two Iranian hospitals. Mycopathologia. 2021;186:519-33.
3. Pérez-Cantero A, López-Fernández L, Guarro J, Capilla J. Azole resistance mechanisms in Aspergillus: update and recent advances. International Journal of Antimicrobial Agents. 2020;55(1):105807.

4. Vahedi-Shahandashti R, Lass-Flörl C. Novel Antifungal Agents and Their Activity against Aspergillus Species. J Fungi (Basel). 2020;6(4).
5. Hosseinikargar N, Basiri R, Asadzadeh M, Najafzadeh MJ, Zarrinfar H. First report of invasive Aspergillus rhinosinusitis in a critically ill COVID-19 patient affected by acute myeloid leukemia, northeastern Iran. Clinical case reports. 2021;9(10).
6. Nourizadeh N, Adabizadeh A, Zarrinfar H, Majidi M, Jafarian AH, Najafzadeh MJ. Fungal biofilms in sinonasal polyposis: the role of fungal agents is notable? Journal of Oral and Maxillofacial Surgery, Medicine, and Pathology. 2019;31(4):295-8.
7. Zakaria A, Osman M, Dabboussi F, Rafei R, Mallat H, Papon N, et al. Recent trends in the epidemiology, diagnosis, treatment, and mechanisms of resistance in clinical Aspergillus species: A general review with a special focus on the Middle Eastern and North African region. J Infect Public Health. 2020;13(1):1-10.
8. Arastehfar A, Carvalho A, Houbraken J, Lombardi L, Garcia-Rubio R, Jenks J, et al. Aspergillus fumigatus and aspergillosis: From basics to clinics. Studies in mycology. 2021;100(1):100115-.
9. Paulussen C, Hallsworth JE, Álvarez-Pérez S, Nierman WC, Hamill PG, Blain D, et al. Ecology of aspergillosis: insights into the pathogenic potency of Aspergillus fumigatus and some other Aspergillus species. Microb Biotechnol. 2017;10(2):296-322.
10. Hossain CM, Ryan LK, Gera M, Choudhuri S, Lyle N, Ali KA, et al. Antifungals and Drug Resistance. Encyclopedia. 2022;2(4):1722-37.
11. Fisher MC, Alastruey-Izquierdo A, Berman J, Bicanic T, Bignell EM, Bowyer P, et al. Tackling the emerging threat of antifungal resistance to human health. Nature Reviews Microbiology. 2022;20(9):557-71.
12. Dehghani R, Mohammadi S, Zarrinfar H, Jarahi L, Najafzadeh MJ, Salah H. The emergence of decreased activity of amphotericin B and voriconazole against clinical isolates of Aspergillus species: a subtropical region of the Middle East. Journal of Population Therapeutics and Clinical Pharmacology. 2023;30(17):146-54.
13. Khojasteh S, Abastabar M, Haghani I, Valadan R, Ghazanfari S, Abbasi K, et al. Five-year surveillance study of clinical and environmental Triazole-Resistant Aspergillus fumigatus isolates in Iran. Mycoses. 2023;66(2):98-105.
14. Jenks JD, Hoenigl M. Treatment of Aspergillosis. J Fungi (Basel). 2018;4(3).
15. McKeny PT, Nessel TA, Zito PM. Antifungal antibiotics. StatPearls [Internet]: StatPearls Publishing; 2022.
16. Zhen C, Lu H, Jiang Y. Novel Promising Antifungal Target Proteins for Conquering Invasive Fungal Infections. Frontiers in Microbiology. 2022;13:911322.
17. Menezes RdP, Bessa MAdS, Siqueira CdP, Teixeira SC, Ferro EAV, Martins MM, et al. Antimicrobial, Antivirulence, and Antiparasitic Potential of Capsicum chinense Jacq. Extracts and Their Isolated Compound Capsaicin. Antibiotics. 2022;11(9):1154.
18. Kowalska J, Tyburski J, Krzymińska J, Jakubowska M. Cinnamon powder: an in vitro and in vivo evaluation of antifungal and plant growth promoting activity. European Journal of Plant Pathology. 2020;156:237-43.
19. Xi K-Y, Xiong S-J, Li G, Guo C-Q, Zhou J, Ma J-W, et al. Antifungal Activity of Ginger Rhizome Extract against Fusarium solani. Horticulturae. 2022;8(11):983.
20. Archana H, Bose VG. Evaluation of phytoconstituents from selected medicinal plants and its synergistic antimicrobial activity. Chemosphere. 2022;287:132276.
21. Simonetti G, Brasili E, Pasqua G. Antifungal Activity of Phenolic and Polyphenolic Compounds from Different Matrices of Vitis vinifera L. against Human Pathogens. Molecules. 2020;25(16).
22. Adamczak A, Ożarowski M, Karpiński TM. Curcumin, a natural antimicrobial agent with strain-specific activity. Pharmaceuticals. 2020;13(7):153.
23. Akter J, Amzad Hossain M, Sano A, Takara K, Zahorul Islam M, Hou D-X. Antifungal Activity of Various Species and Strains of Turmeric (Curcuma SPP.) Against Fusarium Solani Sensu Lato. Pharmaceutical Chemistry Journal. 2018;52(4):320-5.

24. Jennings MR, Parks RJ. Curcumin as an Antiviral Agent. Viruses. 2020;12(11).
25. Naderi MJJ, Mahmoudi A, Kesharwani P, Jamialahmadi T, Sahebkar A. Recent advances of nanotechnology in the treatment and diagnosis of polycystic ovary syndrome. Journal of Drug Delivery Science and Technology. 2022:104014.
26. Nagargoje AA, Akolkar SV, Siddiqui MM, Subhedar DD, Sangshetti JN, Khedkar VM, et al. Quinoline based monocarbonyl curcumin analogs as potential antifungal and antioxidant agents: Synthesis, bioevaluation and molecular docking study. Chemistry & Biodiversity. 2020;17(2):e1900624.
27. Shaker B, Ahmad S, Lee J, Jung C, Na D. In silico methods and tools for drug discovery. Computers in biology and medicine. 2021;137:104851.
28. Meylani V, Putra RR, Miftahussurur M, Sukardiman S, Hermanto FE, Abdullah A. Molecular docking analysis of Cinnamomum zeylanicum phytochemicals against Secreted Aspartyl Proteinase 4–6 of Candida albicans as anti-candidiasis oral. Results in Chemistry. 2023;5:100721.
29. Shrivastava M, Sharma P, Singh R. Identification of potential CYP51 inhibiting anti-Aspergillus phytochemicals using molecular docking and ADME/T studies. Chemical Biology Letters. 2021;8(1):18-21.
30. Robbins N, Caplan T, Cowen LE. Molecular evolution of antifungal drug resistance. Annual review of microbiology. 2017;71:753-75.
31. UniProt: the universal protein knowledgebase. Nucleic Acids Res. 2017;45(D1):D158-d69.
32. Sofi M, Shafi A, Masoodi K. Chapter 22-Introduction to computer-aided drug design. Bioinformatics for everyone. 2022:215-29.
33. Waterhouse A, Bertoni M, Bienert S, Studer G, Tauriello G, Gumienny R, et al. SWISS-MODEL: homology modelling of protein structures and complexes. Nucleic acids research. 2018;46(W1):W296-W303.
34. Wiltgen M. Algorithms for Structure Comparison and Analysis: Homology Modelling of Proteins. In: Ranganathan S, Gribskov M, Nakai K, Schönbach C, editors. Encyclopedia of Bioinformatics and Computational Biology. Oxford: Academic Press; 2019. p. 38-61.
35. Sahay A, Piprodhe A, Pise M. In silico analysis and homology modeling of strictosidine synthase involved in alkaloid biosynthesis in catharanthus roseus. Journal of Genetic Engineering and Biotechnology. 2020;18:1-6.
36. Guruprasad K, Reddy BV, Pandit MW. Correlation between stability of a protein and its dipeptide composition: a novel approach for predicting in vivo stability of a protein from its primary sequence. Protein Eng. 1990;4(2):155-61.
37. Ikai A. Thermostability and aliphatic index of globular proteins. J Biochem. 1980;88(6):1895-8.
38. Kyte J, Doolittle RF. A simple method for displaying the hydropathic character of a protein. J Mol Biol. 1982;157(1):105-32.
39. Agnihotry S, Pathak RK, Singh DB, Tiwari A, Hussain I. Chapter 11 - Protein structure prediction. In: Singh DB, Pathak RK, editors. Bioinformatics: Academic Press; 2022. p. 177-88.
40. Silakari O, Singh PK. Chapter 5 - Homology modeling: Developing 3D structures of target proteins missing in databases. In: Silakari O, Singh PK, editors. Concepts and Experimental Protocols of Modelling and Informatics in Drug Design: Academic Press; 2021. p. 107-30.
41. Irwin JJ, Sterling T, Mysinger MM, Bolstad ES, Coleman RG. ZINC: a free tool to discover chemistry for biology. Journal of chemical information and modeling. 2012;52(7):1757-68.
42. Kim S, Thiessen PA, Bolton EE, Chen J, Fu G, Gindulyte A, et al. PubChem substance and compound databases. Nucleic acids research. 2016;44(D1):D1202-D13.
43. Bertoni M, Kiefer F, Biasini M, Bordoli L, Schwede T. Modeling protein quaternary structure of homo-and hetero-oligomers beyond binary interactions by homology. Scientific reports. 2017;7(1):1-15.
44. Kontoyianni M. Docking and virtual screening in drug discovery. Proteomics for drug discovery: Methods and protocols. 2017:255-66.

45. Dallakyan S, Olson AJ. Small-molecule library screening by docking with PyRx. Chemical biology: methods and protocols. 2015:243-50.
46. Pettersen EF, Goddard TD, Huang CC, Couch GS, Greenblatt DM, Meng EC, et al. UCSF Chimera—a visualization system for exploratory research and analysis. Journal of computational chemistry. 2004;25(13):1605-12.
47. Biovia DS. Discovery studio modeling environment. Release; 2017.
48. Daina A, Michielin O, Zoete V. SwissADME: a free web tool to evaluate pharmacokinetics, drug-likeness and medicinal chemistry friendliness of small molecules. Scientific reports. 2017;7(1):42717.
49. Noe M, Peakman M-C. Drug discovery technologies: Current and future trends. 2017.
50. Banerjee P, Eckert AO, Schrey AK, Preissner R. ProTox-II: a web server for the prediction of toxicity of chemicals. Nucleic acids research. 2018;46(W1):W257-W63.
51. Pires DE, Blundell TL, Ascher DB. pkCSM: predicting small-molecule pharmacokinetic and toxicity properties using graph-based signatures. Journal of medicinal chemistry. 2015;58(9):4066-72.
52. Pokharkar O, Lakshmanan H, Zyryanov G, Tsurkan M. In Silico Evaluation of Antifungal Compounds from Marine Sponges against COVID-19-Associated Mucormycosis. Mar Drugs. 2022;20(3).
53. Xu C, Cheng F, Chen L, Du Z, Li W, Liu G, et al. In silico prediction of chemical Ames mutagenicity. J Chem Inf Model. 2012;52(11):2840-7.
54. Borba JVB, Alves VM, Braga RC, Korn DR, Overdahl K, Silva AC, et al. STopTox: An in Silico Alternative to Animal Testing for Acute Systemic and Topical Toxicity. Environ Health Perspect. 2022;130(2):27012.
55. Filimonov D, Lagunin A, Gloriozova T, Rudik A, Druzhilovskii D, Pogodin P, et al. Prediction of the biological activity spectra of organic compounds using the PASS online web resource. Chemistry of Heterocyclic Compounds. 2014;50:444-57.
56. Cheminformatics M. Nova ulica, SK-900 26 Slovensky Grob, Slovak Republic. 2018.
57. Biasini M, Bienert S, Waterhouse A, Arnold K, Studer G, Schmidt T, et al. SWISS-MODEL: modelling protein tertiary and quaternary structure using evolutionary information. Nucleic acids research. 2014;42(W1):W252-W8.
58. Ahmad W, Ansari MA, Alsayari A, Almaghaslah D, Wahab S, Alomary MN, et al. In Vitro, Molecular Docking and In Silico ADME/Tox Studies of Emodin and Chrysophanol against Human Colorectal and Cervical Carcinoma. Pharmaceuticals. 2022;15(11):1348.
59. Latgé J-P, Chamilos G. Aspergillus fumigatus and Aspergillosis in 2019. Clinical microbiology reviews. 2019;33(1):e00140-18.
60. Sugui JA, Kwon-Chung KJ, Juvvadi PR, Latgé JP, Steinbach WJ. Aspergillus fumigatus and related species. Cold Spring Harb Perspect Med. 2014;5(2):a019786.
61. Zhang J, Li L, Lv Q, Yan L, Wang Y, Jiang Y. The Fungal CYP51s: Their Functions, Structures, Related Drug Resistance, and Inhibitors. Front Microbiol. 2019;10:691.
62. Pérez-Cantero A, Martin-Vicente A, Guarro J, Fortwendel JR, Capilla J. Analysis of the cyp51 genes contribution to azole resistance in Aspergillus section Nigri with the CRISPR-Cas9 technique. Antimicrob Agents Chemother. 2023;65(5).
63. Geißel B, Loiko V, Klugherz I, Zhu Z, Wagener N, Kurzai O, et al. Azole-induced cell wall carbohydrate patches kill Aspergillus fumigatus. Nature communications. 2018;9(1):3098.
64. Roundtree MT, Juvvadi PR, Shwab EK, Cole DC, Steinbach WJ. Aspergillus fumigatus Cyp51A and Cyp51B proteins are compensatory in function and localize differentially in response to antifungals and cell wall inhibitors. Antimicrobial Agents and Chemotherapy. 2020;64(10):e00735-20.
65. Gonzalez-Jimenez I, Lucio J, Amich J, Cuesta I, Sanchez Arroyo R, Alcazar-Fuoli L, et al. A Cyp51B mutation contributes to azole resistance in Aspergillus fumigatus. Journal of Fungi. 2020;6(4):315.

66. Hargrove TY, Garvey EP, Hoekstra WJ, Yates CM, Wawrzak Z, Rachakonda G, et al. Crystal structure of the new investigational drug candidate VT-1598 in complex with Aspergillus fumigatus sterol 14α-demethylase provides insights into its broad-spectrum antifungal activity. Antimicrobial agents and chemotherapy. 2017;61(7):e00570-17.
67. Cao D, Yao S, Zhang H, Wang S, Jin X, Lin D, et al. Mutation in cyp51A and high expression of efflux pump gene of Aspergillus fumigatus induced by propiconazole in liquid medium and soil. Environmental Pollution. 2020;256:113385.
68. Dudakova A, Spiess B, Tangwattanachuleeporn M, Sasse C, Buchheidt D, Weig M, et al. Molecular Tools for the Detection and Deduction of Azole Antifungal Drug Resistance Phenotypes in Aspergillus Species. Clin Microbiol Rev. 2017;30(4):1065-91.
69. Paul RA, Rudramurthy SM, Dhaliwal M, Singh P, Ghosh AK, Kaur H, et al. Magnitude of Voriconazole Resistance in Clinical and Environmental Isolates of Aspergillus flavus and Investigation into the Role of Multidrug Efflux Pumps. Antimicrob Agents Chemother. 2018;62(11).
70. de Wit K, Paulussen C, Matheeussen A, van Rossem K, Cos P, Maes L. In vitro profiling of pramiconazole and in vivo evaluation in Microsporum canis dermatitis and Candida albicans vaginitis laboratory models. Antimicrob Agents Chemother. 2010;54(11):4927-9.
71. Geria AN, Scheinfeld NS. Pramiconazole, a triazole compound for the treatment of fungal infections. IDrugs. 2008;11(9):661-70.
72. Sahni K, Singh S, Dogra S. Newer Topical Treatments in Skin and Nail Dermatophyte Infections. Indian Dermatol Online J. 2018;9(3):149-58.
73. Hussain Y, Alam W, Ullah H, Dacrema M, Daglia M, Khan H, et al. Antimicrobial Potential of Curcumin: Therapeutic Potential and Challenges to Clinical Applications. Antibiotics (Basel). 2022;11(3).
74. Neelofar K, Shreaz S, Rimple B, Muralidhar S, Nikhat M, Khan LA. Curcumin as a promising anticandidal of clinical interest. Can J Microbiol. 2011;57(3):204-10.
75. Azari B, Zahmatkesh Moghadam S, Zarrinfar H, Tasbandi A, Jamialahmadi T, Sahebkar A. Antifungal Activity of Curcuminoids and Difluorinated Curcumin Against Clinical Isolates of Candida Species. Adv Exp Med Biol. 2021;1328:123-9.
76. Chen E, Benso B, Seleem D, Ferreira LEN, Pasetto S, Pardi V, et al. Fungal-Host Interaction: Curcumin Modulates Proteolytic Enzyme Activity of Candida albicans and Inflammatory Host Response In Vitro. Int J Dent. 2018;2018:2393146.
77. Alalwan H, Rajendran R, Lappin DF, Combet E, Shahzad M, Robertson D, et al. The Anti-Adhesive Effect of Curcumin on Candida albicans Biofilms on Denture Materials. Front Microbiol. 2017;8:659.
78. Sadeghi-Ghadi Z, Vaezi A, Ahangarkani F, Ilkit M, Ebrahimnejad P, Badali H. Potent in vitro activity of curcumin and quercetin co-encapsulated in nanovesicles without hyaluronan against Aspergillus and Candida isolates. Journal de Mycologie Medicale. 2020;30(4):101014.
79. Ma J, Shi H, Sun H, Li J, Bai Y. Antifungal effect of photodynamic therapy mediated by curcumin on Candida albicans biofilms in vitro. Photodiagnosis and Photodynamic Therapy. 2019;27:280-7.
80. Momtazi AA, Sahebkar A. Difluorinated Curcumin: A Promising Curcumin Analogue with Improved Anti-Tumor Activity and Pharmacokinetic Profile. Curr Pharm Des. 2016;22(28):4386-97.
81. Meccatti VM, Santos LF, de Carvalho LS, Souza CB, Carvalho CAT, Marcucci MC, et al. Antifungal Action of Herbal Plants' Glycolic Extracts against Candida Species. Molecules. 2023;28(6).
82. Dong HH, Wang YH, Peng XM, Zhou HY, Zhao F, Jiang YY, et al. Synergistic antifungal effects of curcumin derivatives as fungal biofilm inhibitors with fluconazole. Chem Biol Drug Des. 2021;97(5):1079-88.

83. Zarrinfar H, Behnam M, Hatamipour M, Sahebkar A. Antifungal Activities of Curcuminoids and Difluorinated Curcumin Against Clinical Dermatophyte Isolates. Adv Exp Med Biol. 2021;1308:101-7.